Seismic resistance of exterior beam-column joints with non-conventional confinement reinforcement detailing

Bindhu, K.R.[†]

Department of Civil Engineering, College of Engineering, Thiruvananthapuram, 695 016, Kerala, India

Jaya, K.P.[‡]

Structural Engineering Division, Anna University, 600 025, Chennai, India

Manicka Selvam, V.K.[‡†]

Department of Civil Engineering, National Institute of Technology, Calicut, Kerala, India

Abstract. The failure of reinforced concrete structures in recent earthquakes caused concern about the performance of beam column joints. Confinement of joint is one of the ways to improve the performance of beam column joints during earthquakes. This paper describes an experimental study of exterior beam-column joints with two non-conventional reinforcement arrangements. One exterior beam-column joint of a six story building in seismic zone III of India was designed for earthquake loading. The transverse reinforcement of the joint assemblages were detailed as per IS 13920:1993 and IS 456:2000 respectively. The proposed non-conventional reinforcement was provided in the form of diagonal reinforcement on the faces of the joint, as a replacement of stirrups in the joint region for joints detailed as per IS 13920 and as additional reinforcement for joints detailed as per IS 456. These newly proposed detailing have the basic advantage of reducing the reinforcement congestion at the joint region. In order to study and compare the performance of joint with different detailing, four types of one-third scale specimens were cast (two numbers in each type). The main objective of the present study is to investigate the effectiveness of the proposed reinforcement detailing. All the specimens were tested under reverse cyclic loading, with appropriate axial load. From the test results, it was found that the beam-column joint having confining reinforcement as per IS: 456 with non-conventional detailing performed well. Test results indicate that the non-conventionally detailed specimens, Type 2 and Type 4 have an improvement in average ductility of 16% and 119% than their conventionally detailed counter parts (Type1 and Type 3). Further, the joint shear capacity of the Type 2 and Type 4 specimens are improved by 8.4% and 15.6% than the corresponding specimens of Type 1 and Type 3 respectively. The present study proposes a closed form expression to compute the yield and ultimate load of the system. This is accomplished using the theory of statics and the failure pattern observed during testing. Good correlation is found between the theoretical and experimental results.

Keywords: beam-column joint; confinement; cyclic loading; design; detailing; equilibrium; seismic analysis; strong column-weak beam.

† Lecturer, Corresponding author, E-mail: bindhukr@yahoo.co.in
‡ Assistant Professor, E-mail: jayakp@annauniv.edu
‡† Retired Professor

1. Introduction

Buildings subjected to seismic forces may undergo several reversals of stresses in the course of an earthquake. Beam-column joint is the critical region in moment resisting frames. Due to the restriction of space available in the joint block, detailing of reinforcement assumes great significance. One of the basic assumptions of frame analysis is that the joints are strong enough to sustain the forces (moments, axial and shear forces) generated by the loading, and to transfer the forces from one structural element to another (beam to column, in most of the cases) (Subramanian and Rao 2003). The assumption of rigidity of joints often ignores the effects of high shear forces developed within them. Actually, the shear failure is always brittle in nature and cannot be deemed an acceptable structural performance especially during earthquakes. Thus, a proper understanding of the joint behavior is imperative in designing earthquake-resistant joints.

In Indian Code of Construction Practice (IS 456:2000), the joint is usually neglected for specific design and attention is restricted to the provision of sufficient anchorage for beam longitudinal reinforcement. This may be acceptable when the frame is not subjected to earthquake loads. Often, the poor design of beam column joints is compounded by the high demand imposed by the adjoining flexural members (beams and columns) in the event of mobilizing their inelastic capacities to dissipate seismic energy. Unsafe design and detailing within the joint region jeopardizes the entire structure, even if other structural members conform to the design requirements. Among the Indian codes IS 13920:1993 deals with the ductile detailing of reinforced concrete structures subjected to seismic forces. However, despite the significance of the joints in sustaining large deformations and forces during earthquakes, specific guidelines or recommendations on beam-column joint are not included in the Indian codes of practice (IS 456:2000 and IS 13920:1993).

According to the capacity design philosophy, beam hinging (while avoiding column hinging and joint shear failure) is the most desirable mode of failure to guarantee high energy dissipation during earthquakes, through significant inelastic deformation and without overall reduction of strength. The implementation of design philosophy presents serious problems particularly in quantifying the different types of damage (structural and non-structural) and what constitutes frequently minor, seldom moderate, and rarely major earthquakes. Plastic hinges are "expected" at locations where structural damage can be allowed to occur due to inelastic actions involving large deformations. Hence, in seismic design, damages in the form of plastic hinges are accepted to form in beams rather than in columns (Uma and Prasad 2006). Proper confinement of joint can be done to rectify the column hinging or joint shear failure. To satisfy the strong column-weak beam collapse mechanism, it is important to understand the progress of damage and failure pattern in joints under seismic loads. This can be obtained by reverse cyclic loading test.

In the past three decades extensive research has been carried out for studying the behavior of joints under seismic conditions (Jisra J.O. 1991). Various international codes have been subjected to periodic revisions. The role of transverse reinforcement and mechanism of shear transfer in the joint for seismic resistance is the subject of much debate (Hwang *et al.* 2005). IS 13920:1993 assumes that the role of hoops is to confine the joint core. The real function of hoops may be both to confine the joint core and to carry shear as tension tie and hence to reduce the width of the crack. The special confining reinforcement (IS 13920:1993) serves three purposes: It provides shear resistance to the member; it confines the concrete core and thereby increases the ultimate strain of concrete, which gives greater ductility to the concrete cross section and enables it to undergo large deformations; it also provides lateral restraint against buckling of the compression reinforcements. Experimental

studies reveal that the usage of the rectangular spiral reinforcement significantly improves the seismic capacity of external beam-column connections (Karayannis *et al.* 2005).

2. Previous research for performance of structural elements related with detailing of reinforcements

Experiments at the University of Canterbury (Park and Paulay 1975) have revealed that the ductility and strength of short coupling beams are improved if the principal reinforcements are placed diagonally instead of horizontally as is done conventionally. The design of such reinforcement is based on the assumption that the shear force resolves itself into diagonal tension and compression. Initially, the diagonal compression is transmitted by concrete and the compression reinforcement makes no significant contribution. When diagonal tension bars are loaded to yield range, wide cracks are formed and these cracks remain open even after the removal of loading. When the reverse load is applied as during an earthquake, these bars are subjected to large compressive force and may yield even before the previous cracks are closed. As equal amount of steel was provided in both the diagonal bands, the loss of contribution of concrete will not affect the strength of the beam. Thus the use of inclined reinforcement prevents brittle failure in short coupling beams. Minami and Wakabayashi (1984) applied the above idea in short columns and found better performance than those with conventional reinforcement. Beam-column joints have many similarities in geometry, state of stress and mechanical behavior with short columns and coupling beams. Durrani and Wight (1985) carried out experiments on interior beam-column joints having lower amount of transverse reinforcement than currently recommended. The authors found that a combination of lower joint shear stress and a moderate amount of joint reinforcement was more effective than a combination of a higher shear stress level and a heavily reinforced joint. Tsonos *et al.* (1992) conducted tests on external beam-column connections using inclined reinforcing bars. The four intermediate vertical joint shear reinforcements were replaced by four cross-inclined bars bent diagonally across the joint core. The development length for both types of bars was equal. The authors found that the exterior joint with inclined bars had higher shear resistance than code recommendations. Also, there was no diagonal cleavage fracture. Tsonos (2000) has investigated the improvement of earthquake resistance of exterior reinforced concrete beam column connection with vertical hoops in the joint region. The results were compared with the response of similar specimens constructed with the vertical joint shear reinforcement required by Eurocode 8 and NZS 3101:82. The author concluded that the vertical joint hoop reinforcement is a more effective reinforcing pattern for sustaining the vertical joint shear force than the intermediate column bars. Bakir and Boduroglu (2002) developed a methodology for predicting the failure modes of monotonically loaded reinforced concrete beam-column joints. The authors concluded that the design charts gave accurate predictions of failure modes. Murty *et al.* (2003) explained the importance of carefully designing beam column joints for the satisfactory performance during strong seismic shaking of R.C framed buildings. They conducted experiments on exterior beam-column joints by changing the anchorage detailing pattern of beam reinforcement and providing hairclip-type bends as confining reinforcement. The authors found that the beam reinforcement with ACI Standard hook and hairclip-type bend stirrup at joint region was the preferred combination. Bakir (2003) conducted a parametric study on shear resisting mechanism of exterior joint using experimental database. A design equation for joint shear force was developed by considering the effect of inclined bars. The author concluded that this equation was an improvement on existing code recommendations. Tsonos (2004)

conducted an experimental study to estimate the improvement of the earthquake resistance of R.C beam-column joints with inclined bars under the influence of *P-Δ* effect. An analytical model was developed for predicting the ultimate shear strength of the beam column joint subjected to earthquake-type loading, variable axial load and *P-Δ* effect. The axial load change and *P-Δ* effect causes significant deterioration of the joint element. The author concluded that the inclined bars in the joint region were effective for reducing the unfavorable impact of *P-Δ* effect and axial load change. Jing *et al.* (2004) conducted experiment on interior joints by changing the beam reinforcement-detailing pattern at the joint core. Diagonal steel bars in the form of "obtuse Z" were installed in two opposite direction of the joint. The authors found that the non-conventional pattern provided was suitable for the joints in regions of low to moderate seismicity. Bakir and Boduroglu (2005) applied nonlinear softened truss model for membrane elements on beam-column joints incorporating the effect of bond slip. The authors suggested that the revised model gives very accurate predictions of shear strength of joints. Tsonos (2007) studied experimentally the performance of beam-column sub assemblages of modern structures. The test results indicate that current design procedures could sometimes lead to excessive damage of the joint regions.

Several researchers have studied the influence of axial load on joint behaviour under cyclic lateral loading. Uzumeri (1977) tested exterior beam-column sub assemblages under high constant axial compressive forces and concluded that the large axial compressive force applied to the concrete struts was detrimental to joint. Bonacci and Pantazopoulou (1993) conducted parametric investigation of interior joint mechanics based on variables such as axial load, amount of transverse reinforcement, concrete strength, presence of transverse beams and bond demand on the strength. The authors found that subject to the scatter of experimental joint shear stress value, the axial load has no discernible coherent influence on the strength of beam-column joints. Algabian *et al.* (1994) tested three interior beam-column subassemblages with ten, five and zero per cent axial load capacity. Test result indicated that the overall displacement response of the subassemblages decreased by 22 per cent for a decrease in the axial load from ten to five per cent of the squash load. Chalioris *et al.* (2008) studied the effectiveness of cross inclined bars as joint shear reinforcement in exterior reinforced concrete beam-column connections under cyclic deformations. The authors suggested that the influence of the column axial load on the shear capacity of the joints is considered to be favorable since the developed principal stresses in the joint are reduced due to the application of compressive axial load, whereas they reach maximum values when the column axial load is nil or insignificant. From the above studies, it can be seen that the effect of axial load on behaviour of joint is to be verified.

From the literatures reviewed it seems that the major role of the stirrup is to resist the shear force in the joint core. The forces in the diagonal confinement bars can be resolved into horizontal and vertical forces to equilibrate the joint shear force. In spite of the wide accumulation of test data the influence of cross inclined bars on shear strength of the joint has not been mentioned in major international codes. Hence in the present work, the confining reinforcement provided also includes two pairs of cross inclined bars which form the X-type reinforcement (Figs. 2 and 4).

3. Objective and problem statement

The aim of the present work is to carry out an experimental investigation to study the effect of non-conventional detailing patterns, in the behavior of reinforced cement concrete beam-columns

joints, under reverse lateral cyclic loading. The proposed non-conventional reinforcement was provided in the form of diagonal reinforcement on the faces of the joint, as a replacement for stirrups in the joint region for joint assemblages with transverse reinforcement detailing as per IS 13920 and as an additional reinforcement for joint assemblages with transverse reinforcement detailing as per IS 456 and including U bars as per SP 34. The newly proposed detailing have the basic advantage of reducing the reinforcement congestion at the joint region. The detailing of transverse reinforcement at the joint was chosen as the major variable parameter for the present study. The effect of axial load on joint behavior was also considered. Based on the failure pattern, expressions for computing yield and ultimate load of the system have been derived. The behavior of the non-conventionally detailed specimens was compared with the conventionally detailed specimens as per Indian Standards (i.e., IS 13920:1993 and IS 456:2000).

3.1 Analysis and design of R.C beam-column joint

A six- storey R.C building located at Chennai, India (in seismic zone III as per IS 1893:2002) on medium soil was analyzed. The shear forces, bending moments and axial forces around the exterior beam column joint due to induced earthquake loading was estimated. Seismic analysis was performed using equivalent lateral force method given in IS 1893:2002 (Jain and Murty 2005a). The design was carried out based on the proposed amendments to IS 1893 and IS 13920 (Ingle and Jain 2005). The transverse reinforcement detailing of beam, column and exterior joint were done by considering ductile detailing as per IS 13920:1993 for the first case and detailing criteria of IS 456:2000 and including additional U bars as per SP 34 for the second case.

3.2 Description of specimens

The specimens were classified into four groups with two numbers in each group. The Type 1 specimens (A1-13920 and A2-13920) were cast with transverse reinforcement detailing as per IS 13920: 1993.The Type 2 specimens (X1-13920 and X2-13920) were detailed as per IS 13920:1993 and the non-conventional reinforcement. One additional stirrup was provided at the middle of the joint to avoid the buckling of longitudinal reinforcement in Type 2 specimens. The Type 3 specimens (A1-456 and A2-456) were detailed as per IS 456: 2000. The Type 4 specimens (X1-456 and X2-456) were cast with the detailing as per IS 456:2000 and the non-conventional reinforcement. The non-conventional reinforcement was provided as two inclined bars on both faces of the joint. The percentage of diagonal bars provided was the same as that of confinining reinforcement required at the joint as per IS 13920: 1993. Care was taken to provide the adequate development length as per the code requirement. All the eight specimens were tested under constant axial load with cyclic load at the end of the beam. One of the specimens from each group was subjected to an axial load of three per cent of column axial load capacity and the other specimen was subjected to an axial load of ten per cent of column axial load capacity (Karayannis *et al.* 2008 Chalioris *et al.* 2008).

The dimensions of the joint, diameter of reinforcement and alignment of longitudinal reinforcement of column were in accordance with the proposed amendments in IS 13920 (Jain and Murty 2005b). The longitudinal reinforcement at the column region and beam region of the specimens were checked for strong column weak beam theory. High yield strength deformed bars were used for the longitudinal reinforcement and high yield strength round bars were used for
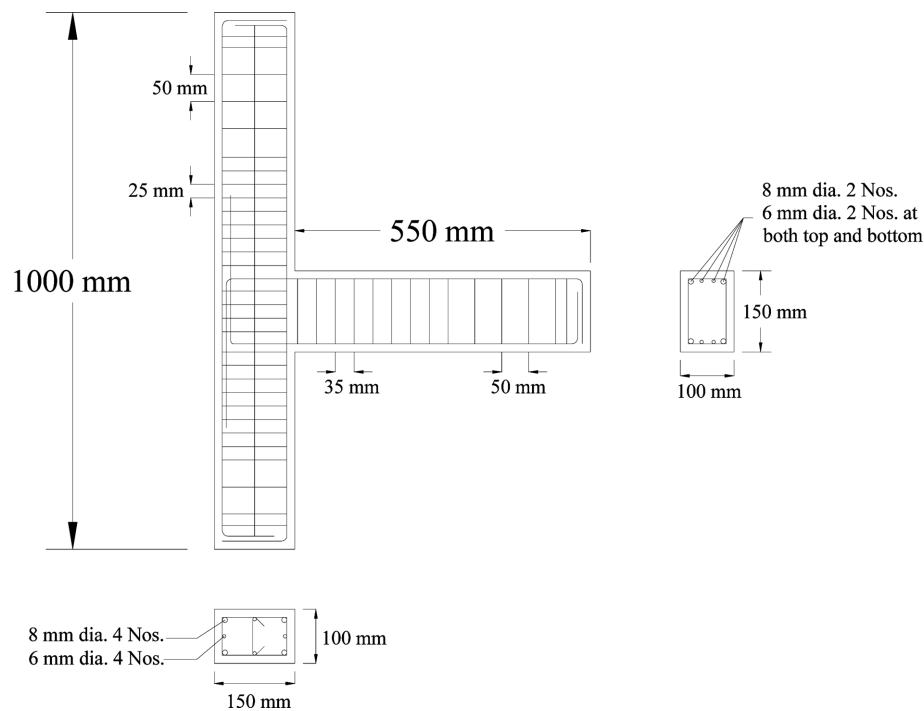
Fig. 1 Reinforcement details of the beam-column joint specimen as per IS 13920
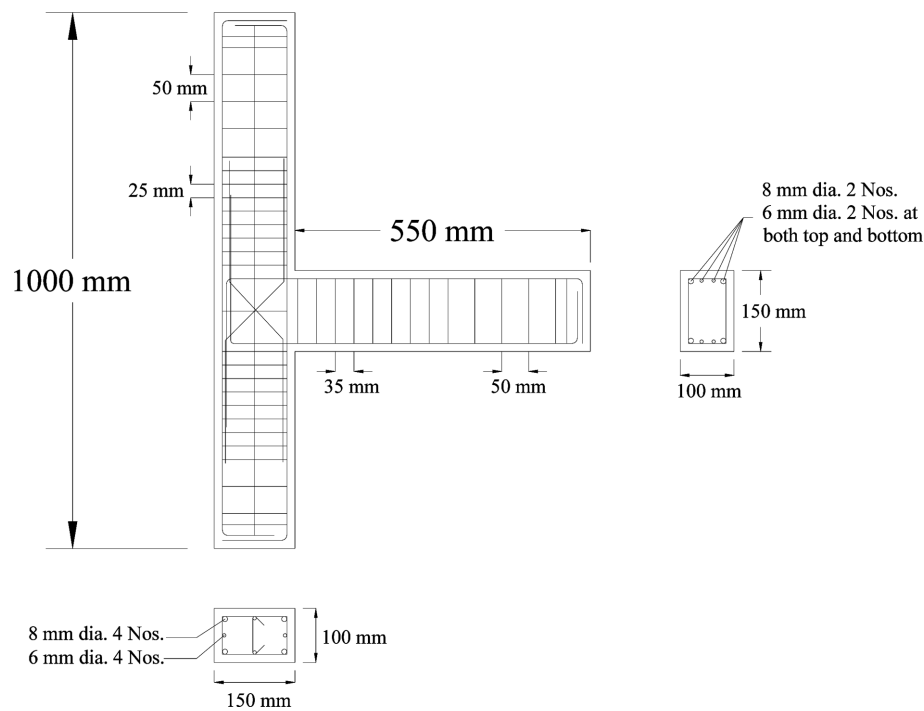
Fig. 2 Reinforcement details of the beam-column joint specimen as per IS 13920 with diagonal confining bars
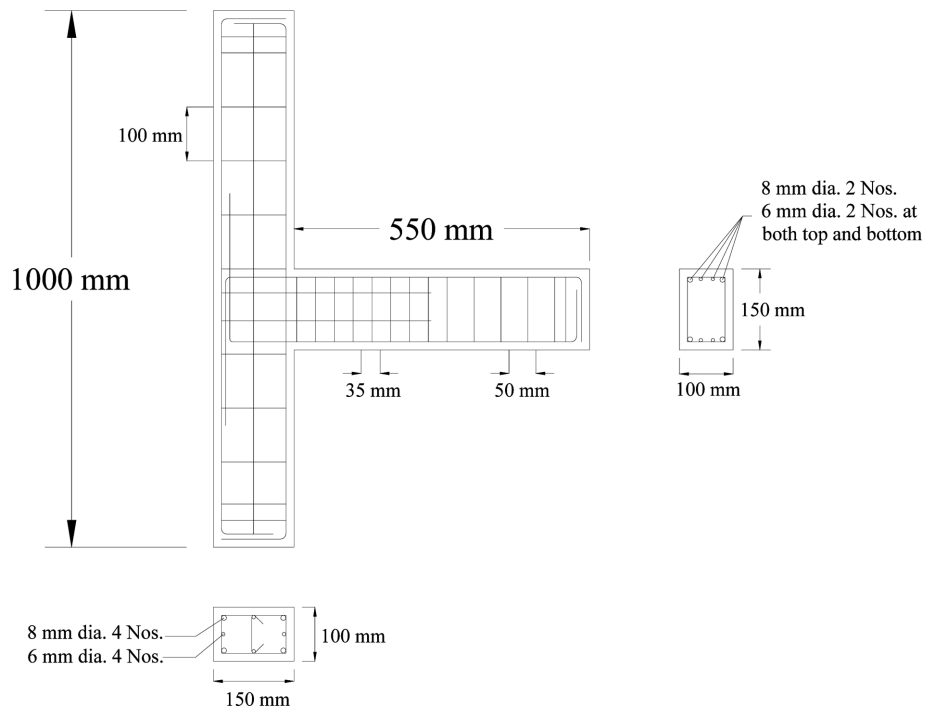
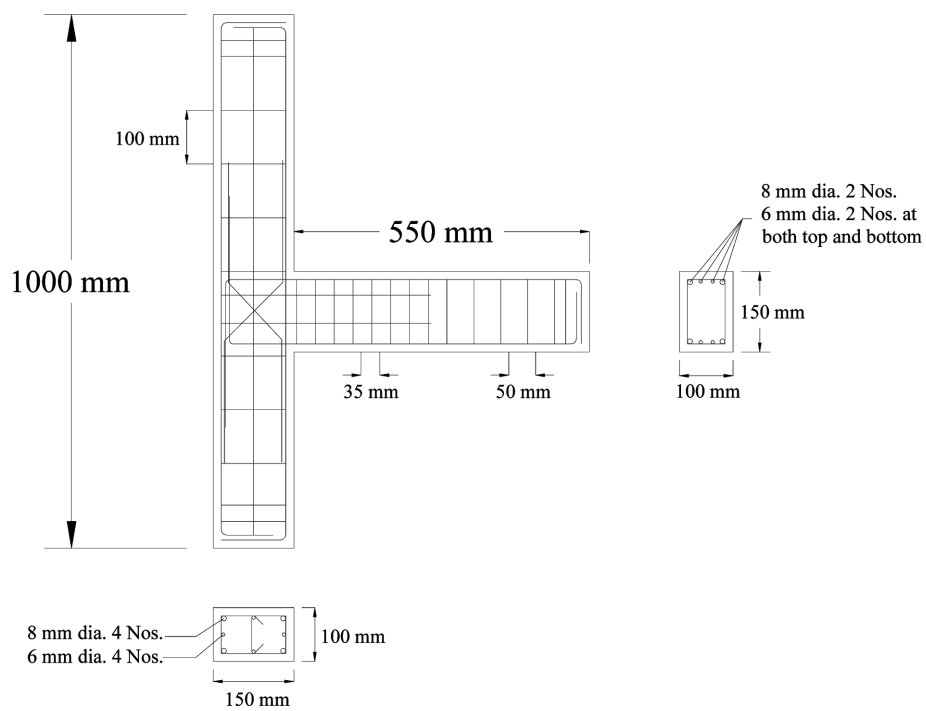Fig. 3 Reinforcement details of the beam-column joint specimen as per IS 456

Fig. 4 Reinforcement details of the beam-column joint specimen as per IS 456 with diagonal confining bars

Table 1 Reinforcement details of test specimens

Specimen designation	Column		Beam		Joint	Remarks
	Longitudinal Reinforcement	Transverse Reinforcement	Longitudinal Reinforcement	Transverse Reinforcement	Transverse Reinforcement	
A1-13920 and A2-13920	4 Φ8, and 4 Φ6.	Φ3 at 25 mm centre to centre for a distance of 230 mm at either side of joint and 50 mm centre to centre for remaining portion	2 Φ8 and 2 Φ6 (top and bottom)	Φ3 at 35 mm centre to center for a distance of 270 mm from joint and 50 mm centre to center for remaining length.	Φ3 at 25 mm centre to centre	Confining reinforcement at joint is as per IS 13920:1993
X1-13920 and X2-13920	4 Φ8, and 4 Φ6.	Φ3 at 25 mm centre to centre for a distance of 230 mm at either side of joint and 50 mm centre to centre for remaining portion	2 Φ8 and 2 Φ6 (top and bottom)	Φ3 at 35 mm centre to centre for a distance of 270 mm from joint and 50 mm center to center for remaining length.	1 Φ3 lateral and 2 Φ6 diagonally on two faces with development length in tension extended to upper and lower column	Confining reinforcement at joint is as per minimum requirement in column, and additional diagonal bars on two faces
A1-456 and A2-456	4 Φ8, and 4 Φ6.	Φ3 at 100 mm centre to centre	2 Φ8 and 2 Φ6 (top and bottom)	Φ3 at 35 mm centre to centre for a distance of 270 mm from joint and 50 mm center to center for remaining length.	Two U bars, Φ3 are provided with development length in tension extended to beam	No stirrups at joint. But two U bars (hairclip-type bend) used for confinement as per IS: 456:2000 & SP34:1987
X1-456 and X2-456	4 Φ8, and 4 Φ6.	Φ3 at 100 mm centre to centre	2 Φ8 and 2 Φ6 (top and bottom)	Φ3 at 35 mm centre to centre for a distance of 270 mm from joint and 50 mm centre to centre for remaining length.	Two U bar, Φ3 as per IS 456 and 2 Φ6 diagonally on two faces with development length in tension extended to upper and lower column	No stirrups at joint. But two U bar (hairclip-type bend) used for confinement as per IS:456: 2000 & SP34:1987 and additional diagonal bars on two faces

stirrups. The column was rectangular in shape with dimensions 100 mm × 150 mm and the beam with dimensions 100 mm × 150 mm with an effective cover of 15 mm in all specimens. The details of the joint assemblage specimens are shown in Fig. 1 to Fig. 4 and in Table 1.

3.3 Casting of specimens

The specimens were cast using ordinary Portland cement (53 grade) conforming to IS 12269: 1987. River sand (medium type) passing through 4.75 mm IS sieve and having a fineness modulus of 2.77 was used as fine aggregate. Crushed granite stone of maximum size not exceeding 8 mm and having a fineness modulus of 3.58 was used as coarse aggregate. The mix proportion was 1: 0.87:1.32 by weight and the water-cement ratio was kept as 0.48. The 28-day average compressive strength from 150 mm cube test was 44.22 N/mm^2. The yield stress of reinforcement was 432 N/mm^2. All the specimens were cast in horizontal position inside a steel mould on the same day. Specimens were demoulded after 24 hours and then cured under wet gunny bags for 28 days.

4. Experimental set up

The joint assemblages were subjected to axial and reverse cyclic load. The specimens were tested in an upright position and static reverse cyclic loading was applied at the end of the beam. A constant column axial load was applied by means of 392.4 kN (40 t) hydraulic jack mounted vertically to the 981 kN (100 t) loading frame to simulate the gravity load on the column. The axial load was selected as three and ten per cent of the column axial load capacities for the first and second series respectively. Axial load for the first series specimen was 15.92 kN (1.62 t) and for the second series was 53.06 kN (5.41 t). One end of the column was given an external hinge support, which was fastened to the strong reaction floor, and the other end was laterally restrained by a roller support to allow moment-free rotation at both ends. A schematic drawing of the setup is shown in Fig. 5. Cyclic loading was applied by two 196.2 kN (20 t) hydraulic jacks, one kept fixed to the loading frame and the other to the strong reaction floor. Reverse cyclic load was applied at 50 mm from the free end of the beam portion of the assemblage. The test was load- controlled and the specimen was subjected to an increasing cyclic load up to failure. The load increment chosen was 1.962 kN (200 kg). The specimen was first loaded up to 1.962 kN and unloaded and then reloaded on the reverse direction up to 1.962 kN. The subsequent cycles were also loaded in a similar way. To record loads precisely, load cells with least count 0.0981 kN were used. The specimens were instrumented with Linear Variable Differential Transformer (LVDT) having least count 0.1 mm to measure the deflection at the loading point. Electrical resistance strain gauges were used to measure the strain in the reinforcement during testing. The experimental setup at laboratory is shown in Fig. 6.

5. Cracking pattern and failure mode

In all the specimens in the first series (with axial load 15.92 kN), initial diagonal hairline crack on the joint occurred at the second loading cycle when the load reached 3.924 kN in both positive and negative cycle of loading. But for the second series (with axial load 53.06 kN), the first crack
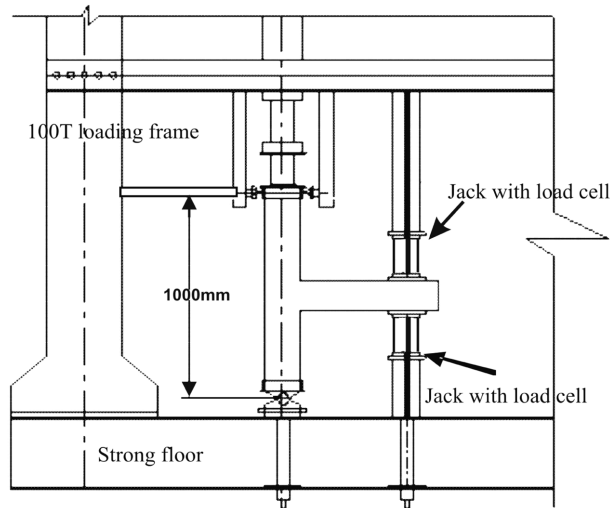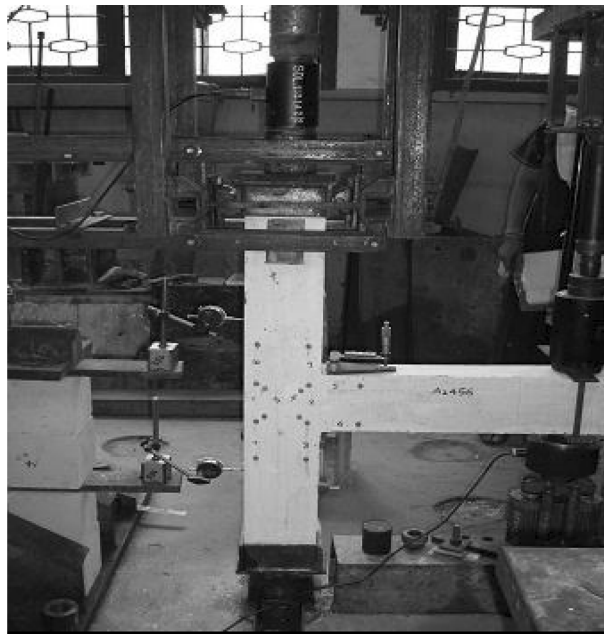
Fig. 5 Schematic diagram of test set-up

Fig. 6 Test setup in the Laboratory

appeared only in the third cycle for a load of 5.886 kN in all specimens. The yield and ultimate load for the test specimens are shown in Table 2. The cracking patterns of test specimens in the first and second series are shown in Fig. 7 and Fig. 8. In almost all specimens tensile cracks were developed at the interface between the column and beam. Extensive damage at the joint region can be noticed in specimen A1-13920 (Fig. 7(a)), but when axial load increases the damage gets reduced as seen in A2-13920 (Fig. 8 (a)). The specimens failed due to the advancement of crack width at the interface between beam and column. There was a clear vertical cleavage formed at the

Table 2 Yield and ultimate load of specimens from experiment

Designation of specimen	Experimental Yield Load (kN)			Experimental Ultimate Load (kN)		
	Downward direction	Upward direction	Average (P_{ye})	Downward direction	Upward direction	Average (P_{ue})
A1-13920	11.77	11.77	11.77	16.18	15.69	15.93
X1-13920	13.73	13.73	13.73	18.63	17.65	18.14
A1-456	15.69	13.73	14.71	16.67	14.71	15.69
X1-456	13.73	13.73	13.73	19.62	19.62	19.62
A2-13920	15.7	15.7	15.7	17.65	19.62	18.64
X2-13920	13.73	13.73	13.73	18.64	18.64	18.64
A2-456	15.7	15.7	15.7	18.64	18.64	18.64
X2-456	15.7	13.73	14.71	19.62	19.62	19.62

junction of all the specimens. In addition, for the first series specimens, A1-13920 and A1-456, cracks were developed in the joint region also (Fig. 7 (a) and Fig. 7(c)). But, in the case of X1-13920 and X1-456, the cracks were concentrated in the beam region only (Fig. 7(b) and Fig. 7(d)). Among the specimens, X1-456 exhibited the best performance. The second series specimens were tested under increased axial load. The performance was improved due to the increased axial load. Fig. 8 shows the specimens in the second series. Like in the case of the first series, the specimens had failed due to vertical cleavage at beam-column joint interface.

A major flexural crack was developed at the beam-column interface in all specimens. For the specimens with inclined bars (with non-conventional detailing) no major cracks were noticed at the joint and the joint remained intact throughout the test. Here the failure was dominated by tensile failure at the interface than at the joint failure. The improvement of performance by developing further cracks away from the joint face to the beam region can be noticed for the specimens with U-bars and inclined bars (X1-456 and X2-456). For specimen X2-456 the crack width is also less compared to other specimens.

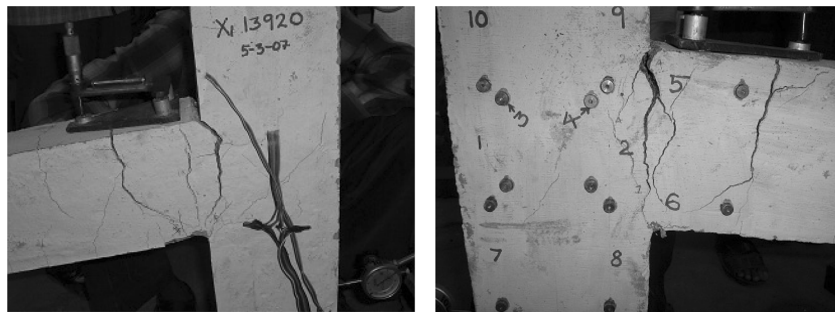## 6. Proposed theoretical analysis

From the experiments conducted on eight specimens, it was observed that at ultimate condition the failure pattern in almost all the systems was same with a clear vertical cleavage at the interface between the column and the beam. Based on this failure pattern, the following description of the force system is propounded as a starting point in order to evaluate the yield load and ultimate load of the system. The supposition proposed for the system of forces at the interface is shown in Fig. 9(b) whereas Fig. 9(a) shows the cleavage in the specimen. The yield force in the reinforcement remains unchanged from the onset of yielding till rupture occurs in concrete, whereas the force in concrete is quite small at the onset of steel yielding and attains its full value at ultimate stage. Because of this fact, the contribution of concrete to the ultimate load is separately computed and added to the yield load, in order to obtain the ultimate load P_u of the subassemblage.

$$\text{i.e., } P_u = P_{ys} + P_{ucon} \tag{1}$$

where P_{ys} is the yield load of steel and P_{ucon} is the concrete contribution to the ultimate load.

(a) Specimen A1-13920

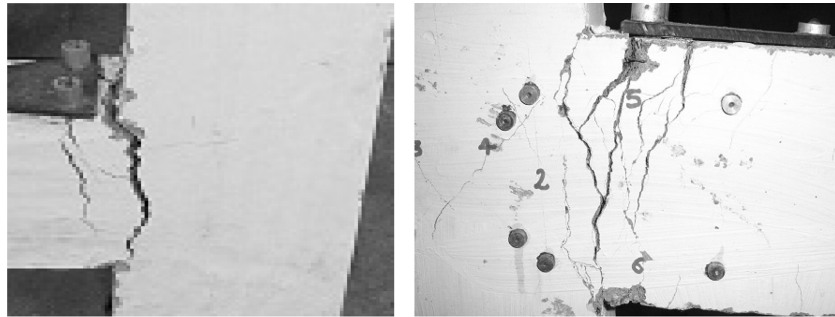(b) Specimen X1-13920

(c) Specimen A1-456

(d) Specimen X1-456

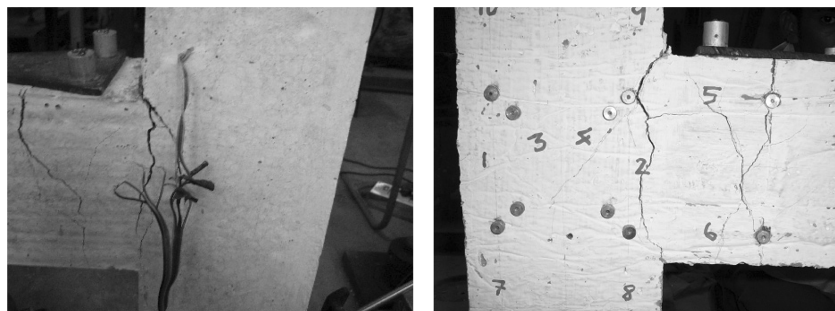Fig. 7 Crack pattern in the specimens of First Series

(a) Specimen A2-13920

(b) Specimen X2-13920

(c) Specimen A2-456

(d) Specimen X2-456
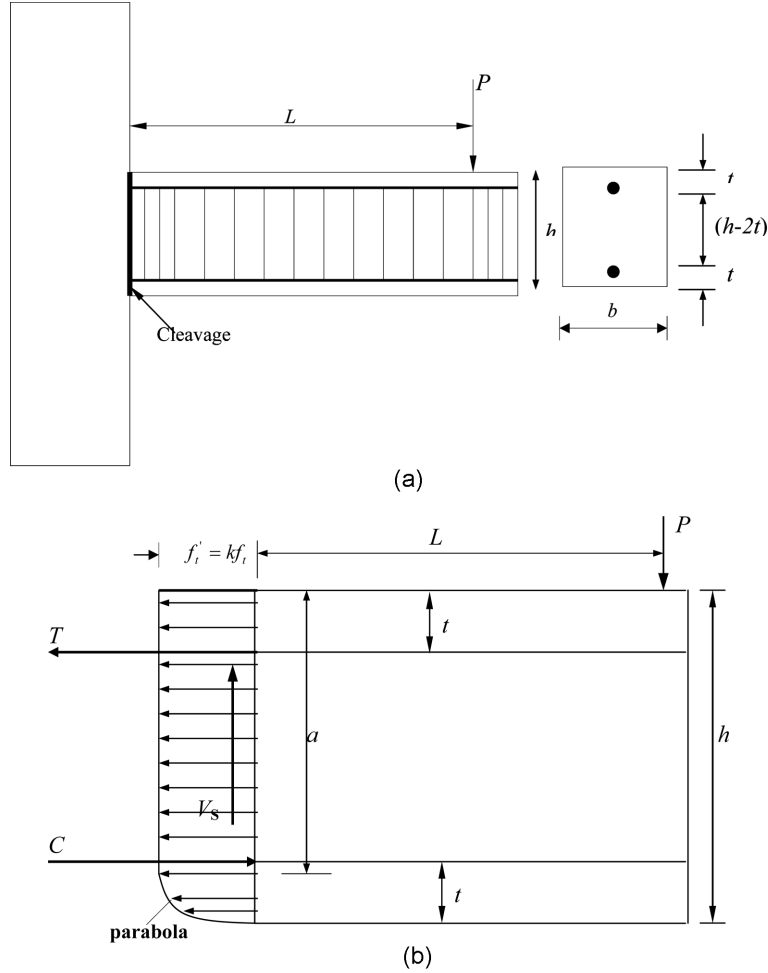
Fig. 8 Crack pattern in the specimens of Second Series

Fig. 9 (a) Cleavage pattern and (b) Force system at failure

The various forces acting on the interface are:

1. A Tensile force in concrete which is assumed as rectangular for a distance "a" from the top edge and parabolic for the remaining portion

$$T_c = baf_t' + \frac{2}{3}b(h-a)f_t'$$

where b = breadth of beam, h = overall depth of beam, f_t' = the tensile stress of concrete.

$f_t' = kf_t$ in which k is a stress reduction factor $0 < k < 1$ and f_t is the maximum tensile stress in concrete.

2. A Tensile yield force in top steel $T = \sigma_y A_{st}$
3. A compressive force in bottom steel $C = \sigma_s A_{st}$
4. A vertical force V_s that consists of a dowel force in steel as well as shear force that arises in concrete.

The unknowns are P, σ_s, and V_s

Now applying the three static equilibrium conditions to the force system shown in Fig. 9(b) gives,

$$\sum H = 0$$

$$T + T_c - C = 0$$

Substituting the value of T_c gives,

$$T + baf_t^{'} + \frac{2}{3}b(h-a)f_t^{'} - C = 0 \tag{2}$$

$$\sum V = 0$$

$$P - V_S = 0 \tag{3}$$

$$\sum M = 0 \quad \text{(Taking moment of all the forces about the bottom steel)}$$

$$P = \frac{1}{L}\left\{ T(h-2t) + \left(ab\left(h-t-\frac{a}{2}\right) + \frac{2}{3}b(h-a)\left(\frac{5}{8}(h-a)-t\right)\right)f_t^{'} \right\} \tag{4}$$

where L = lever arm of the force, t = effective cover of concrete.

The maximum value of "a" is obtained by considering $\dfrac{dP}{da} = 0$ which leads to $a = (h-2t)$. Substituting this value of "a" in Eq. (4) gives

$$P = P_u = \frac{1}{L}\left\{ T(h-2t) + \left(\frac{bh}{2}(h-2t) + \frac{bt^2}{3}\right)f_t^{'} \right\} \tag{5}$$

Eq. (5) is the expression for the ultimate load carrying capacity P_u of the system.

6.1 Principle of virtual displacements

It is an alternative work theory employed for investigating the forces in system, which is in equilibrium. The theorem states:

"If a force system in equilibrium is given an infinitesimal virtual displacement, then the total work done W_e by the forces is equal to zero."

The system has three degrees of freedom, δH, δV, and $\delta \theta$ (two translational and one rotational degree of freedom). The system is given one displacement at a time keeping the other two arrested. Corresponding to each degree of freedom one equilibrium equation is obtained.

(a) The system is subjected to a horizontal displacement δH as shown in Fig. 10(a). Then applying the theorem to the disturbed system

$$W_e = -C\,\delta H + T\,\delta H + baf_t^{'}\,\delta H + \frac{2}{3}b(h-a)f_t^{'}\,\delta H = 0 \tag{6}$$

The sign convention used is that a force is positive if it is acting in the same direction as that of the displacement.

Now, rearranging Eq. (6)

$$C = \left(T + baf_t^{'} + \frac{2}{3}b(h-a)f_t^{'} \right) \tag{7}$$

(b) The system is subjected to a vertical displacement δV (Fig. 10(b)). Then the work equation becomes
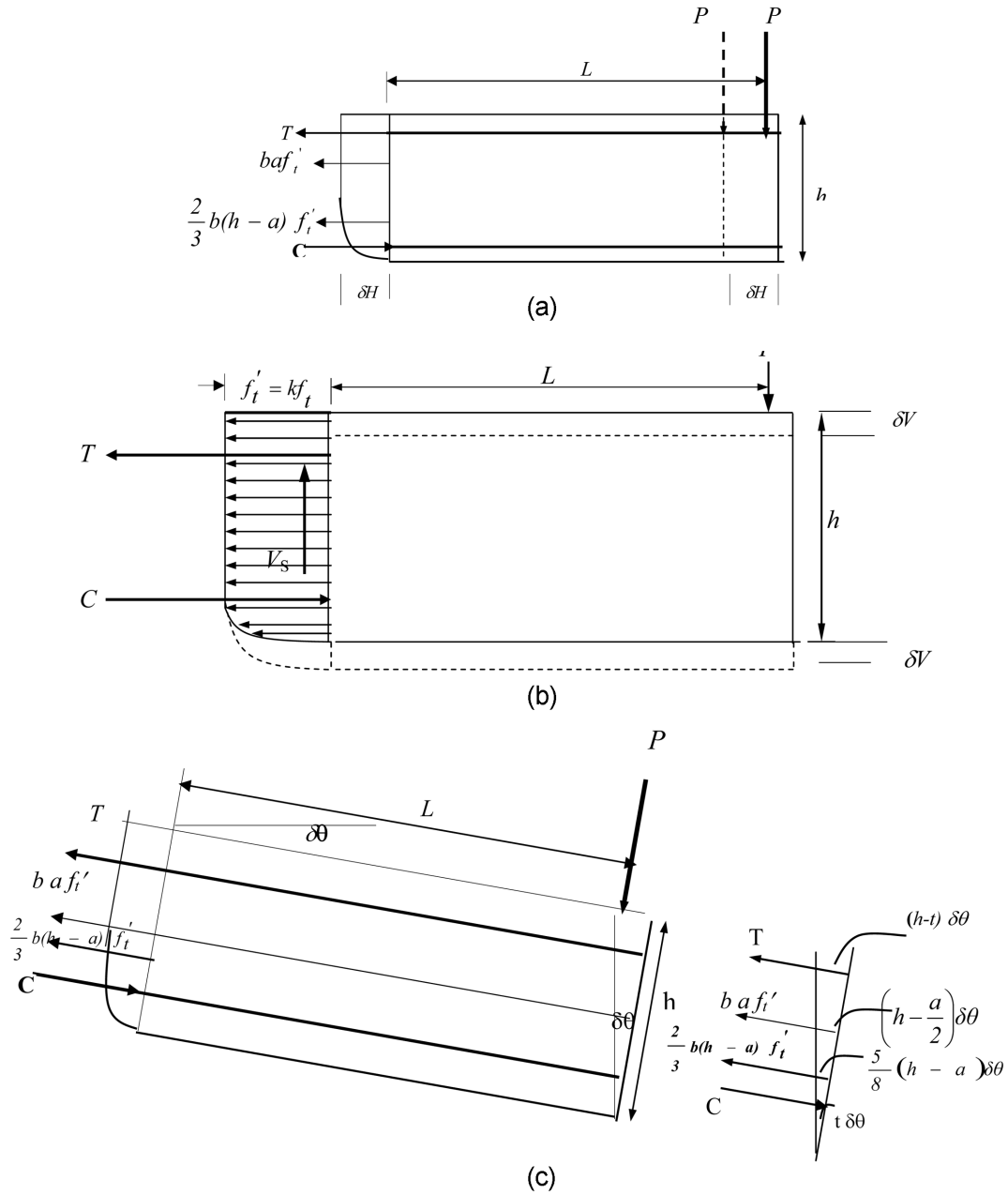
Fig. 10 (a) Horizontal displacement δH, (b) Vertical displacement δV, and (c) Rotational displacement $\delta\theta$

$$V_S \delta V - P\,\delta V = 0$$
$$V_S - P = 0 \tag{8}$$

(c) Here the force system is impressed by a rotational displacement $\delta\theta$ as shown in Fig. 10(c). Application of the theorem to the system gives

$$-T(h-t)\delta\theta - baf_t'\left(h - \frac{a}{2}\right)\delta\theta - \frac{2}{3}b(h-a)f_t'\frac{5}{8}(h-a)\delta\theta + C_t\delta\theta + PL\,\delta\theta = 0$$

Cancelling out $\delta\theta$ through out gives rise to

$$P = \frac{1}{L}\left\{T(h-t) + ba\left(h - \frac{a}{2}\right)f_t' + \frac{10}{24}b(h-a)^2f_t' - Ct\right\} \tag{9}$$

Substituting Eqs. (7) in (9), P can be expressed as

$$P = \frac{1}{L}\left\{T(h-2t) + ba\left(h - \frac{a}{2}\right)f_t' + \frac{10}{24}b(h-a)^2f_t' - \frac{1}{3}btf_t'(a+2h)\right\} \tag{10}$$

Observing $a = (h - 2t)$ obtained by setting $\dfrac{dP}{da} = 0$ as before gives the value of P_u as

$$P = P_u = \frac{1}{L}\left\{T(h-2t) + \left(\frac{bh}{2}(h-2t) + \frac{bt^2}{3}\right)f_t'\right\} \tag{11}$$

It is seen that Eqs. (5) and (11) are identical.

6.2 Determination of the stress reduction factor 'k'

In the case of steel, the yield stress σ_y can be assessed in a more accurate manner. However, there exists considerable difficulty in determining the value of the stress reduction factor 'k'. According to ACI Code formula, the maximum tensile stress in concrete is expressed as:

$$f_t = f_{cr} = 0.623\sqrt{f_c'} \tag{12}$$

where $f_c' = 0.8f_{ck}$ in which f_c' is the cylinder compressive strength, f_{ck} is the characteristic cube strength and f_{cr} is the modulus of rupture of concrete.

When a concrete member is subjected to stresses due to bending moment and shear force, tensile stress at any point is $f_t' = kf_t$. At present sufficient information regarding the magnitude of k is not available. In the absence of reliable data, the stress reduction factor 'k' is taken '*a priori*' as the average value equal to 0.5.

6.3 Load at first yielding of reinforcement

When the steel begins to yield, the development of tensile stress in the concrete is in the incipient stage. Full value of f_t would not have attained at this yielding stage. At present, knowledge is inadequate to express the magnitude of the tensile stress in concrete at the onset of yielding in steel. In the absence of categorical information, it is postulated that the tensile force developed is negligible and it is assumed to be equal to zero. With this premise substituting $f_t' \approx 0$ in Eq. (11) gives rise to the following expression for the yield load P_{yc}

$$P_{yc} = \frac{1}{L}(h - 2t)T \tag{13}$$

Using Eqs. (11) and (13), the ultimate load P_u and the yield load P_{yc} are computed for the eight

Table 3 Prediction of Yield and Ultimate Load by Eqs. (11), (13) and (14)

Designation of specimen	Yield Load (kN)			Ultimate Load (kN)				
	Experimental P_{ye}	Theoretical as per proposed method (Eq. 13) P_{yc}	Validation P_{ye}/P_{yc}	Experimental P_{ue}	Theoretical as per proposed method (Eq. 11) P_{u1}	Theoretical as per proposed method (Eq. 14) P_{u2}	Validation P_{ue}/P_{u1}	Validation P_{ue}/P_{u2}
A1-13920	11.77	16.28	0.72	15.93	19.65	19.06	0.81	0.84
X1-13920	13.73	16.28	0.84	18.14	19.65	19.06	0.92	0.95
A1-456	14.71	16.28	0.90	15.69	19.65	19.06	0.80	0.82
X1-456	13.73	16.28	0.84	19.62	19.65	19.06	1.00	1.03
A2-13920	15.7	16.28	0.96	18.64	19.65	19.06	0.95	0.98
X2-13920	13.73	16.28	0.84	18.64	19.65	19.06	0.95	0.98
A2-456	15.7	16.28	0.96	18.64	19.65	19.06	0.95	0.98
X2-456	14.71	16.28	0.90	19.62	19.65	19.06	1.00	1.03
Mean			0.870	Mean			0.922	0.951
Standard deviation			0.073	Standard deviation			0.072	0.075

$b=100$ mm, $h=150$ mm, $t=15$ mm, $\sigma_y=432$ MPa, $f_{ck}=44.22$ MPa, $f_t' = 0.5f_t$, $f_t = f_{cr} = 0.623\sqrt{f_c'}$, $f_c' = 0.8f_{ck}$, $A_{st}=157.08$ mm^2, $L=500$ mm.

specimens and are tabulated in Table 3. Good correlation between these two, subject to scatter in the results of concrete studies suggests that the hypothesis put forward is justified. Now, the concrete contribution to the ultimate load of the system is computed by another theory, *viz.,* principal stress theory which is delineated below.

6.4 Principal stress theory

Among the failure theories, the principal stress theory is found to give reasonably good solution for brittle materials. Using this theory, the tensile strength contribution by the concrete can be found.

$$\text{The ultimate load } P_u = P_{yc} + P_{ucon} \tag{14}$$

6.4.1 Computation of P_{ucon}

At the interface at the time of yielding in steel, bending moment and shearing force exist in concrete whose distributions are as shown in Fig. 11.

The section is uncracked in the beginning and when yielding in steel just starts the stress distribution in concrete is obtained from Fig. 11. It is seen from Fig. 11, that topmost fibre is subjected to principal tensile stress, i.e.,

$$\sigma_1 = \frac{M}{Z} = \frac{6P_{ucon}L}{bh^2} \tag{15}$$

where σ_1 is the principal tensile stress in concrete, M is the bending moment causing failure of concrete and Z is the section modulus. When σ_1 is equal to the tensile stress f_t as given by ACI code (Eq. 12), rupture occurs in concrete. Substituting various values for b, h, σ_1 and L in Eq. (15) gives the contribution of concrete for the ultimate load carrying capacity as

$$P_{ucon} = 2.78 \text{ kN}$$

From the onset of cracking till the ultimate condition, there is no change in steel strength, which is obtained from Eq. (13) as 16.28 kN. Now the ultimate load from Eq. (14) is obtained as 19.06 kN. The results are tabulated in Table 3.

7. Discussion of results

In this section, the test results are presented in the form of load-deformation hysteretic curves, energy dissipation curves, ductility charts and the force-reinforcement strain envelops. The
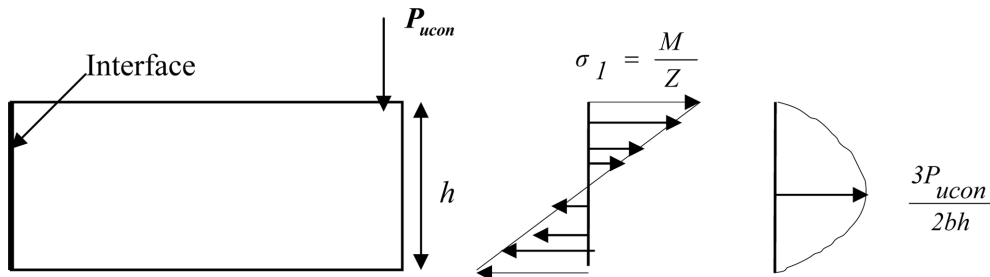

Fig. 11 Flexural and shear stress distribution

observations during the test are briefly described here.

7.1 Hysteretic loops

The force - displacement hysteretic loops for all specimens are as shown in Fig. 12 to Fig. 19. From Table 2, it can be seen that the ultimate load carrying capacity is higher for specimens
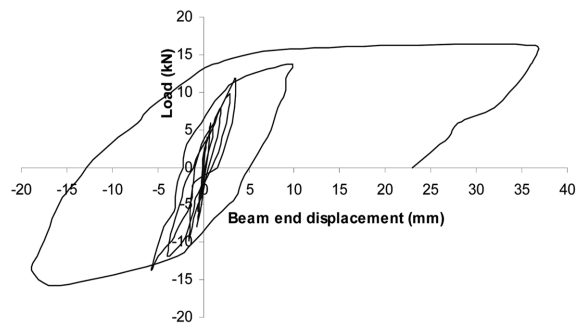

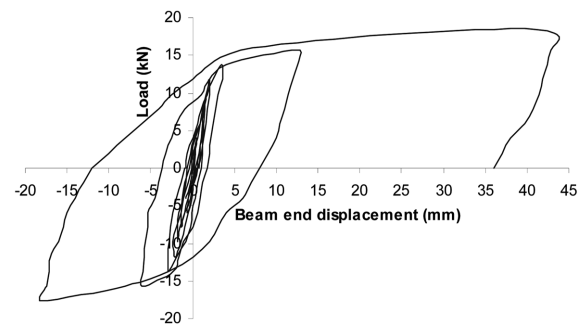Fig. 12 Load versus displacement curve of specimen A1-13920

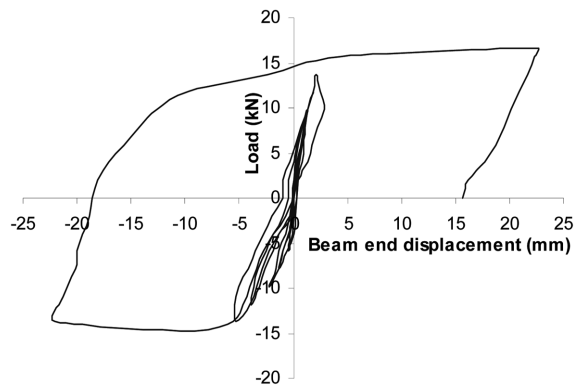Fig. 13 Load versus displacement curve of specimen X1-13920

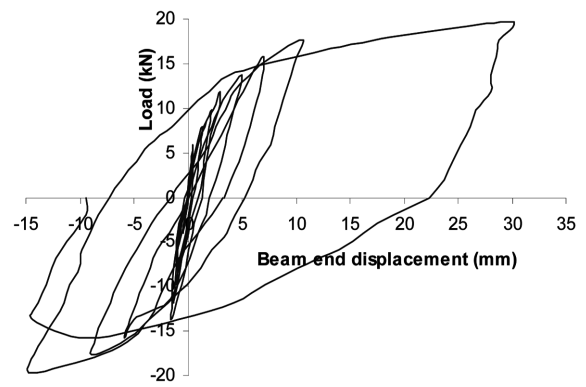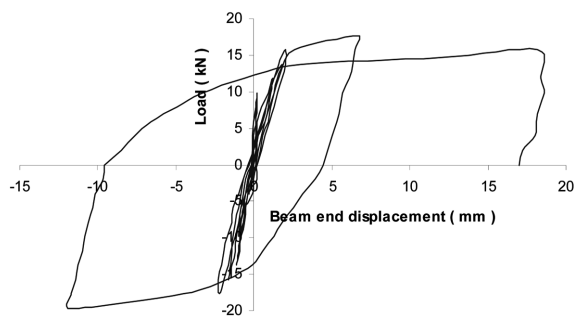

Fig. 14 Load versus displacement curve of specimen A1-456

Fig. 15 Load versus displacement curve of specimen X1-456

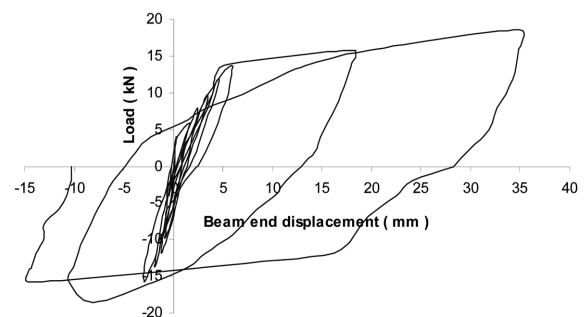Fig. 16 Load versus displacement curve of specimen A2-13920

Fig. 17 Load versus displacement curve of specimen X2-13920
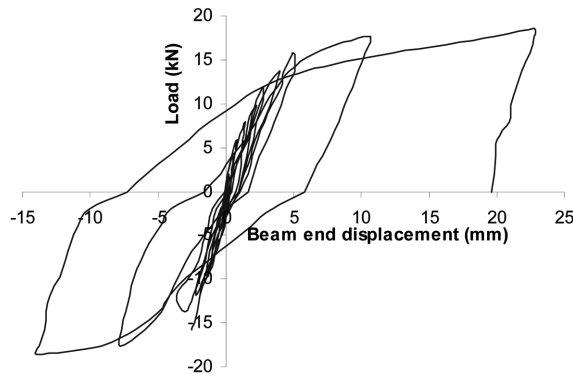
Fig. 18 Load versus displacement curve of specimen A2-456
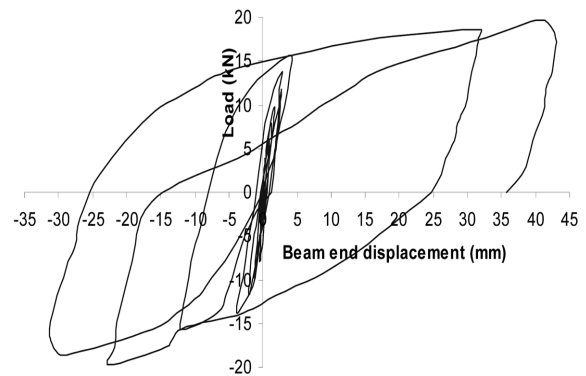

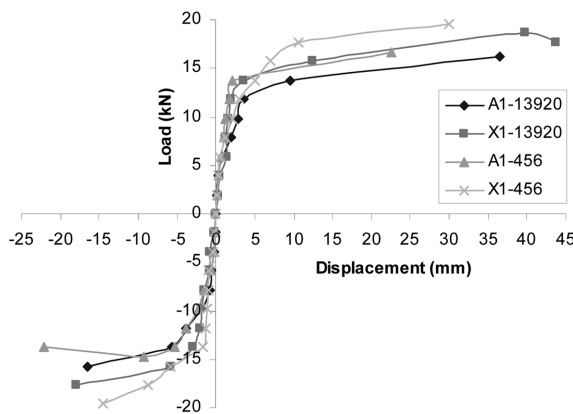Fig. 19 Load versus displacement curve of specimen X2-456

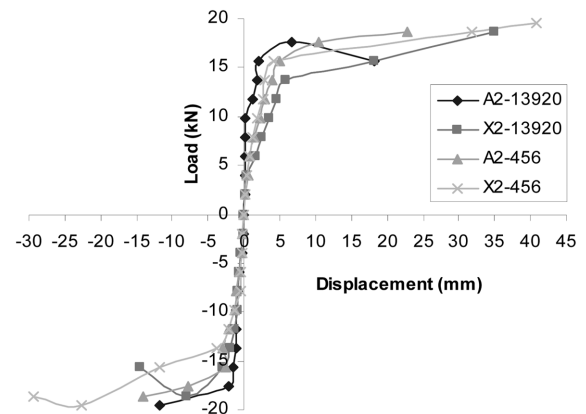Fig. 20 Load-displacement envelopes of specimens in first series

Fig. 21 Load-displacement envelopes of specimens in second series

detailed as per IS 456 with U bars and inclined bars. In this type of non-conventional detailing, the stiffness increases with loading up to seventh cycle. Here the ductility and energy dissipation capacities increased without compromising the stiffness. In general, specimens with inclined bars perform better than conventionally detailed counterparts. A relative comparison of overall force-deformation behavior of all specimens in series 1 and series 2 are as shown in Fig. 20 and Fig. 21 respectively. It is clear that specimen X1-456 and X2-456 attained maximum loads with less strength degradation.

7.2 Energy dissipation

Structures with higher energy dissipation characteristics are able to undergo stronger shaking and exhibit better seismic response. The area enclosed by a hysteretic loop at a given cycle represents the energy dissipated by the specimen during that cycle (El-Amoury and Ghobarah 2002). Fig. 22 shows the cumulative energy dissipated versus cumulative displacement curve of all specimens. It was observed that specimen X2-456 has the highest value of energy dissipation of 2478.74 kN mm. The energy dissipation for all the specimens is shown in Fig. 23. It was observed that the increase
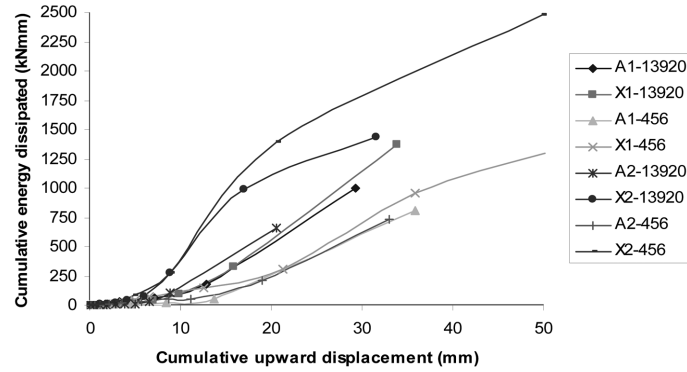
Fig. 22 Cumulative energy dissipation curves of specimens

in axial load is beneficial for improving the energy dissipation characteristics of specimens with inclined bars and U-bars. The energy dissipated in each cycle for the test specimens are shown in Fig. 24 to Fig. 27. It is clearly observed that specimens detailed with inclined bars (the non-conventional detailing) have more energy dissipation than that of conventionally detailed specimens.

7.3 Displacement ductility

Ductility is the capacity of the structure/member to undergo deformation beyond yield without loosing much of the load carrying capacity. In earthquake resistant design of structures, all the critical regions should be designed and detailed with large ductility and stable hysteretic behavior. The ductility is generally measured in terms of displacement ductility, which is the ratio of the maximum deformation that a structure or element can undergo without significant loss of initial yielding resistance to the initial yield deformation (Park and Paulay 1975). The displacement ductility for all specimens are presented in Table 4. The effect of axial load on the displacement ductility can be seen from the ductility bar chart shown in Fig. 28. The series 1 specimen with $0.03 f_c' A_g$ column axial load (where A_g is the gross cross sectional area of column) had higher ductility than the series 2 specimens with $0.1 f_c' A_g$ column axial load. The displacement ductility of
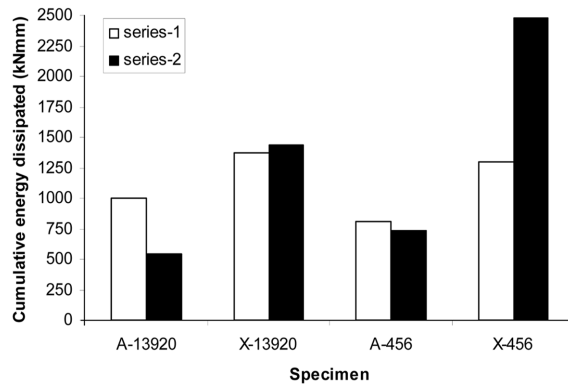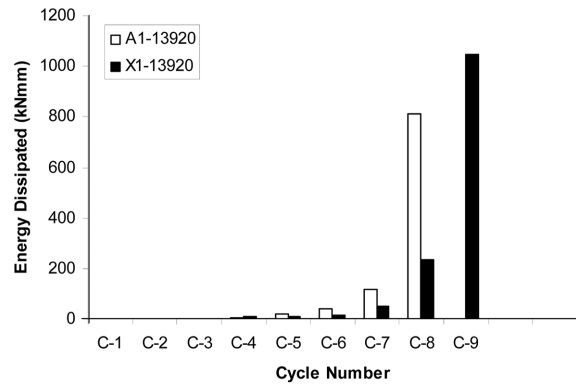

Fig. 23 Energy dissipation chart

Fig. 24 Energy dissipation chart in each cycle for specimens A1-13920 and X1-13920
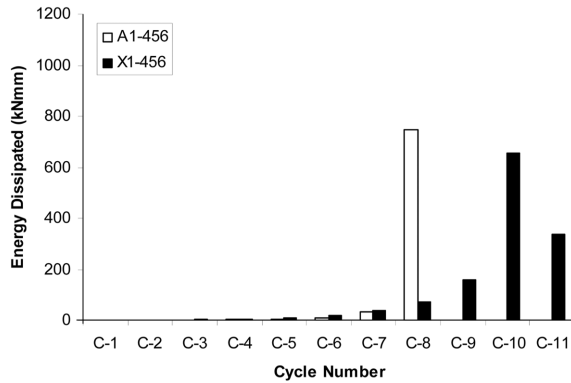
Fig. 25 Energy dissipation chart in each cycle for specimens A1-456 and X1-456
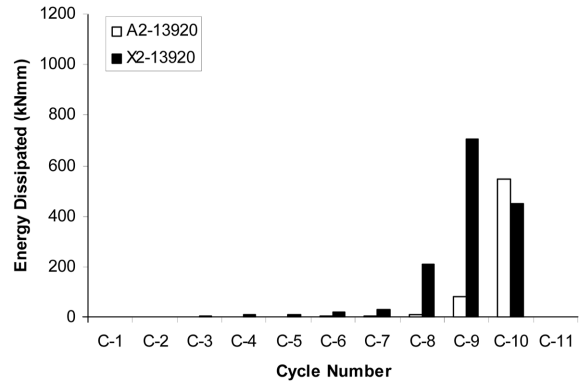

Fig. 26 Energy dissipation chart in each cycle for specimens A2-13920 and X2-13920
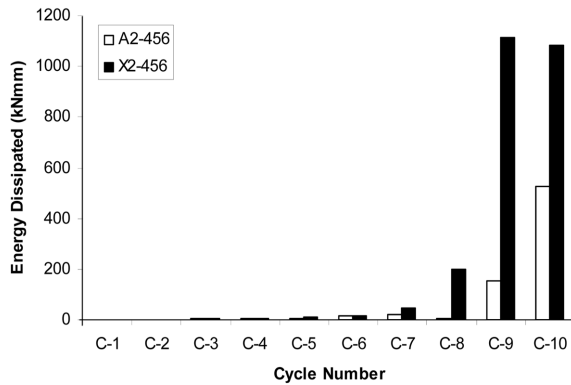

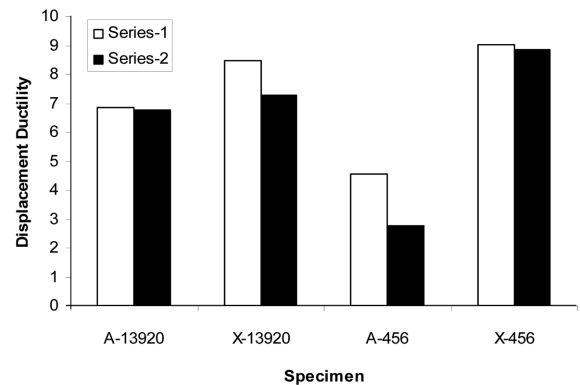Fig. 27 Energy dissipation chart in each cycle for specimens A2-456 and X2-456

Fig. 28 Ductility Bar Chart

Table 4 Displacement ductility of specimens

Specimen	Displacement (mm)				Displacement ductility		Average ductility	% increase of Ductility for Non conventional specimens
	Yield		Ultimate					
	Downward direction	Upward direction	Downward direction	Upward direction	Downward direction	Upward direction		
A1-13920	4.2	3.8	36.5	18.9	8.69	4.97	6.83	-----
X1-13920	4	3	43.7	18	10.93	6	8.46	23.86
A1-456	4.4	5.5	22.6	22.1	5.13	4.01	4.57	-----
X1-456	3.9	1.4	29.9	14.5	7.67	10.35	9.01	97.15
A2-13920	2.6	1.8	18.2	11.8	7	6.56	6.78	-----
X2-13920	5.1	1.9	35	14.6	6.86	7.68	7.27	7.23
A2-456	5	5	22.8	14	4.56	2.8	3.68	-----
X2-456	4.1	2.9	40.8	22.6	9.95	7.79	8.87	141

specimens with inclined bars was found to be higher than their conventionally detailed counter parts. The specimens X1-456 and X2-456 (with inclined bars and U bars) exhibited high displacement ductility.

Table 5 Comparison of Ultimate joint shear stress with ACI code prescribed limiting values

Designation of specimen	Downward Ultimate Load P_uKn	τ_{jh}, MPa	% increase For X-specimen	τ_{jh}/τ_{ACI}	Upward Ultimate Load P_ukN	τ_{jh}, MPa	% increase For X-specimen	τ_{jh}/τ_{ACI}
A1-13920	16.18	6.02	---	1.01	15.69	5.84	---	0.98
X1-13920	18.63	6.94	15.28	1.17	17.65	6.57	12.5	1.10
A1-456	16.67	6.20	---	1.04	14.71	5.47	---	0.92
X1-456	19.62	7.31	17.90	1.23	19.62	7.31	33.64	1.23
A2-13920	17.65	6.57	---	1.10	19.62	7.31	---	1.23
X2-13920	18.64	6.94	5.63	1.17	18.64	6.94	---	1.17
A2-456	18.64	6.94	---	1.17	18.64	6.94		1.17
X2-456	19.62	7.31	5.33	1.23	19.62	7.31	5.33	1.23

$f_c' = 35.376$ MPa, Maximum permissible shear stress τ_{ACI} as per $ACI = 5.92$ MPa.

7.4 Joint shear stress

The horizontal shear stress of the exterior joint sub assemblage can be given by Eq. (16) (Murty *et al.* 2003).

$$\tau_{jh} = \frac{P}{A_{core}^h}\left(\frac{L_b}{d_b} - \frac{L_b + 0.5D_c}{L_c}\right) \tag{16}$$

where P is the imposed cyclic load at the end of the beam; L_b and L_c are lengths of beam and column, respectively; D_c is total depth of column; d_b is effective depth of beam; and A_{core}^h is horizontal cross-sectional area of the joint core resisting the horizontal shear force. It is necessary to limit the magnitude of horizontal joint shear stress to protect the joint against diagonal crushing. The ACI-318 standard limits the horizontal joint shear stress as $0.083\gamma\sqrt{f_c'}$ MPa, where f_c' is the cylinder compressive strength in MPa. The factor γ depends on the confinement provided by the members framing in to the joint; γ is taken as 20, 15 and 12 for interior, exterior, and corner joints, respectively.

The ultimate value of joint horizontal shear stress induced in the joints are almost equal or little higher than the ACI recommended values. It can be seen from Table 5 that the shear resisting capacity is more for non-conventionally detailed specimens than the conventional specimens. The increase in axial load also improves the shear capacity of joints.

7.5 Reinforcement strain

In order to study the effectiveness of non-conventional detailing, electrical resistance strain gauge data for the first series of specimens were measured. The locations of strain gauges are shown in Fig. 29(a). The envelopes of beam end force - reinforcement strain curve are shown in Fig. 29 to Fig. 32. It can be seen that the column bars of the conventionally detailed specimens strained to some extent. But for the non-conventional specimen the strain in column main bars were negligible. The main reinforcement in the outer face of column was free from strains. This indicates that shear damage in the joint region was reduced for these specimens. Strain readings of gauges confirmed
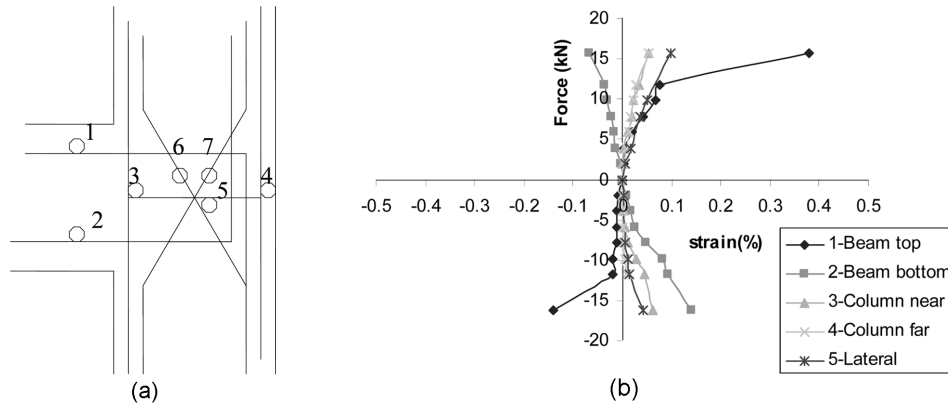
Fig. 29 (a) Locations of strain gauges and (b) Force-reinforcement strains envelope of specimen A1-13920

Fig. 30 Force-reinforcement strains envelope of specimen X1-13920
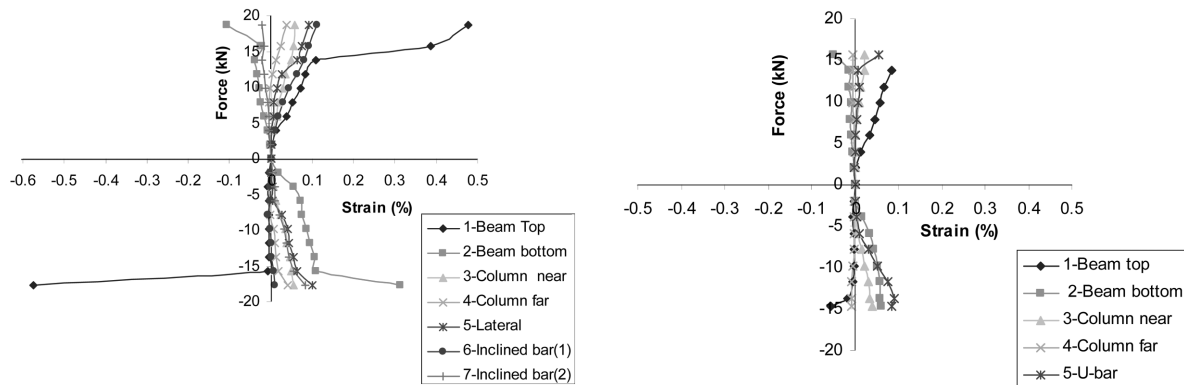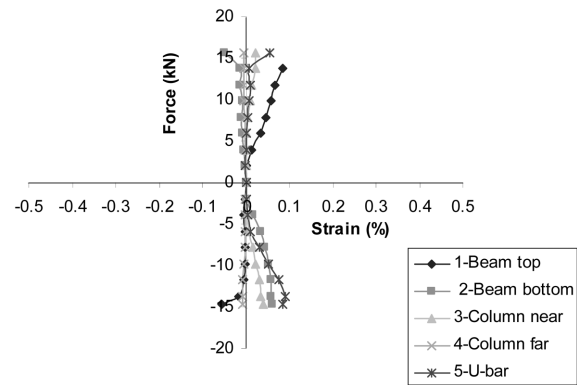

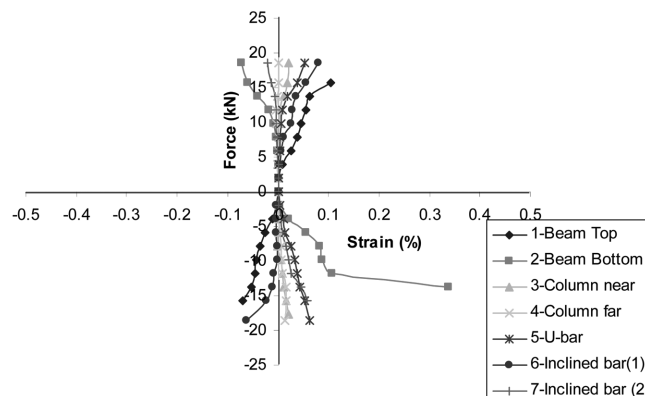Fig. 31 Force-reinforcement strains envelope of specimen A1-456

Fig. 32 Force-reinforcement strains envelope of specimen X1-456

that all column longitudinal bars remained elastic during testing. The inclined bars remained active during the entire cycle and accept the shear stresses. The strains in the beam bars were higher for all the specimens which show the beam mode failure.

8. Conclusions

The experimental study focused on developing non-conventional reinforcement detailing in order to reduce the congestion in the joint region. Eight specimens were cast and tested. The confining reinforcement was detailed as per i) IS 13920 (Type 1, 2Nos), ii) IS 13920 with non-conventional detailing (Type 2, 2Nos), iii) IS 456 (Type 3, 2Nos), and iv) IS 456 with non-conventional detailing (Type 4, 2Nos). The conclusions of the present study are as follows:

1. The performance of the non-conventional specimens (Type 2 and Type 4) has exhibited higher ultimate strength with minimum cracks in the joint. Specimens with inclined bars and hairpin bends as laterals (Type 4) have higher strength with no appreciable deterioration than other types.

2. Specimens with inclined bars and hairpin bends as laterals (Type 4) exhibited an increase in average ductility of 119% than the conventional specimens (Type 3). Meanwhile for the Type 2 specimens the increase in average ductility was 16% than the conventional specimen (Type1).

3. The shear resistance of the specimen X1-456 (Type 4) is found to be higher by 33.64% than the conventional specimen A1-456. The improvement of shear resistance for X1-13920 (Type 2) is 15.28% than the conventional specimen A1-13920. At higher axial loads, the conventional specimens also performed well for shear resistance compared with the non-conventional specimens. The average improvement in shear resistance of Type 2 and Type 4 specimens are 8.4% and 15.6% respectively.

4. For Type 4 specimens, spindle shaped hysteretic loops with high-energy dissipation capacity were obtained. The cumulative energy dissipated for the specimen X2-456 is more than three times the energy dissipation capacity of the conventional specimen, A2-456. The energy dissipation capacity of Type 2 specimen X2-13920 is more than two times that of the conventional joint A2-13920 (Type 1).

5. The increase in column axial load improves the load carrying capacity and stiffens the joints. For the specimens of Type 4, the energy dissipation capacity and ductility were improved with the increased axial load. But the increase in axial load reduces the energy absorption capacity and ductility of conventionally detailed joints.

6. The cracks in specimens X1-456 and X2-456 (Type 4) were extending to the beam region with less crack width thereby fulfilling the objective of obtaining weak beam.

7. The proposed non-conventional detailing is simple compared to the detailing as per IS: 13920.

8. The Type 4 detailing i.e., providing inclined bars and hairpin bends as laterals can be used in the exterior joints of low rise moment resisting frames in low to moderate seismic risk region.

References

ACI Committee 318 (2002), "Building Code Requirements for Structural Concrete (ACI 318-02)", *Am. Conc. Inst.*, Detroit.

Agbabian, M.S., Higazy, E.M., Abdel-Ghaffar, M., and Elnashai, A.S. (1994), "Experimental observations on the seismic shear performance of R/C beam-to-column connections subjected to varying axial column force", *J. Earthq. Eng. Struct. Dynam.*, **23**, 859-876.

Anandavalli, N., Lakshmanan, N., Jayaraman, R., and Thandavamoorthy, T.S. (2005), "Testing and evaluation of full scale beam-column joints of power plant structures", *J. Struct. Eng., SERC, India*, **32**(1), 1-9.

Bakir, P.G. and Boduroglu, M.H. (2002), "Predicting the failure modes of monotonically loaded reinforced

concrete exterior beam-column joints", *Struct. Eng. Mech.*, **14**(3), 307-330.

Bakir, P.G. (2003), "Seismic Resistance and mechanical behavior of exterior beam-column joints with crossed inclined bars", *Struct. Eng. Mech.*, **16**(4), 493-517.

Bakir, P.G. and Boduroglu, M.H. (2006), "Nonlinear analysis of beam-column joints using softened truss model", *Mech. Res. Commun.*, **33**(2), 134-147.

Bonacci, J. and Pantazopoulou, S. (1993), "Parametric investigation of joint mechanics", *ACI Struct. J.*, **90**(1), 61-71.

Chalioris, C.E., Favvata, M.J., and Karayannis, C.G. (2008), "Reinforced concrete beam-column joints with crossed inclined bars under cyclic deformations", *J. Earthq. Eng. Struct. D*, **37**, 881-897.

Durrani, A.J. and Wight, J.K. (1985), "Behavior of interior beam to column connections under earthquake-type loading", *ACI Struct. J.*, **82**(3), 343-349.

El-Amoury, T. and Ghobarah, A. (2002), "Seismic rehabilitation of beam-column joint using GFRP sheets", *Eng. Struct.*, **24**, 1397-1407.

EuroCode8 (2002), "Design of structures for earthquake resistance (draft)", *European Committee for Standardization*, CEN/TC 250/SC8/N317, 87-89.

Hwang, S.J., Lee, H.J., Liao, T.F., Wang, K.C., and Tsai, S.H. (2005), "Role of hoops on shear strength of reinforced concrete beam-column joints", *ACI Struct. J.*, **102**(3), 445-453.

Ingle, R.K. and Jain, S.K. (2005), "Explanatory examples for ductile detailing of R.C buildings", *IITK-GSDMA Project Report on Building Codes*, I IT, Kanpur, India.

IS 13920 (1993), "Indian standard ductile detailing of reinforced concrete structures subjected to seismic forces", *Bureau of Indian Standards*, New Delhi, India.

IS 1893 (Part 1) (2002), "Indian standard criteria for earthquake resistant design of structures", *Bureau of Indian Standards*, New Delhi, India.

IS 456 (2000), "Indian standard plain and reinforced concrete code of practice", *Bureau of Indian Standards*, New Delhi, India.

Jain, S.K. and Murty, C.V.R. (2005a), "Proposed draft provisions and commentary on Indian seismic code IS 1893 (Part 1)", *IITK-GSDMA Project Report on Building Codes*, IIT, Kanpur, India.

Jain, S.K. and Murty, C.V.R. (2005b), "Proposed draft provisions and commentary on ductile detailing of rc structures subjected to seismic forces", *IITK-GSDMA Project Report on Building Codes*, IIT, Kanpur, India.

Jing, L.I., PAM, H.J., and Kwong, F.T.A.U. (2004), "New details of HSC beam-column joints for regions of low to moderate seismicity", *Proc.13th World Conference on Earthquake Engineering, Vancouver*, Canada, Paper No. **449**.

Jisra, J.O. (1991), "Design of beam-column joints for seismic resistance, SP-123", *Am. Conc. Inst.*, Farmington Hills, Michigan.

Karayannis, C.G, Chalioris, C.E., and Sideris, K.K. (1998), "Effectiveness of RC beam-column connections repair using epoxy resin injections", *J. Earthq. Eng.*, **2**, 217-240.

Karayannis, C., Sirkelis, G., and Mavroeidis, P. (2005), "Improvement of seismic capacity of external beam-column joints using continuous spiral shear reinforcement", *Proc. 5^{th}Conference on "Earthquake Resistant Engineering Structures*, (ERES 2005), Skiathos, Greece,147-156.

Karayannis, C.G. and Sirkelis, G.M. (2008), "Strengthening and rehabilitation of RC beam-column joints using carbon-FRP jacketing and epoxy resin injection", *J. Earthq. Eng. Struct. Dynam.*, **37**, 769-790.

Leon, R.T. (1990), "Shear strength and hysteretic behavior of interior beam-column joints", *ACI Struct. J.*, **87**(1), 3-11.

Minami, K. and Wakabayashi, M. (1984), "Strength and ductility of diagonally reinforced concrete columns", *Proc. 8th World Conference on Earthquake Engineering, San Francisco*, 561-568.

Murty, C.V.R., Durgesh, C. Rai, Bajpai, K.K., and Sudhir, K. Jain (2001), "Anchorage details and joint design in seismic R.C frames", *Indian Conc. J.*, 274-280.

Murty, C.V.R., Durgesh, C. Rai, Bajpai, K.K., and Sudhir, K. Jain (2003), "Effectiveness of reinforcement details in exterior reinforced concrete beam column joints for earthquake resistance", *ACI Struct. J.*, **100**(2), 149-155.

NZS 3101 (1995), "Concrete structures standard, Part 1 and 2, Code and commentary on the design of concrete structures," *New Zealand Standard*, New Zealand.

Pantazopoulou, S. and Bonacci, J. (1992), "Consideration of questions about beam-column joints", *ACI Struct. J.*,

89(1), 27-36.

Park, R. and Paulay, T. (1975), *Reinforced Concrete Structure*, Wiley-Inter science publication, New York, 1975.

Paulay, T., Park, R., and Priestley, M.J.N. (1978), "Reinforced concrete beam-column joints under seismic actions", *ACI J.*, **75**, 585-593.

Paulay, T. and Park, R. (1984), "Joints in reinforced concrete frames designed for earthquake resistance", *Research report 84-9, Department of Civil Engineering, University of Canterbury*, Christchurch, New Zealand.

SatishKumar, S.V., Vijaya Raju, B., and Rajaram, G.S.B.V.S. (2002), "Hysteretic behavior of lightly reinforced exterior beam-to-column joint sub-assemblages", *J. Struct. Eng., S.E.R.C., India*, **30**(3), 31-37.

SP34 (1987), "Indian standard Handbook on concrete reinforcement and detailing", *Bureau of Indian Standards*, New Delhi, India.

Subramanian, N. and Rao, P.D.S. (2003), "Seismic design of joints in RC structures-a review," *Indian Conc. J.*, **77**(2), 883-892.

Tsonos, A.G., Tegos, I.G., and Penelis, G. Gr. (1992), "Seismic resistance of Type 2 exterior beam-column joints reinforced with inclined bars", *ACI Struct. J.*, **89**(1), 3-12.

Tsonos, A.G. (1999), "Lateral load response of strengthened reinforced concrete beam-to-column joints", *ACI Struct. J.*, **96**(1), 46-56.

Tsonos, A.G. (2000), "Effect of vertical hoops on the behavior of reinforced concrete beam-column connections", *Euro. Earthq. Eng.*, **2**, 13-26.

Tsonos, A. G. (2004), "Improvement of the earthquake resistance of R/C beam-column joints under the influence of P-Δ effect and axial force variations using inclined bars", *Struct. Eng. Mech.*, **18**(4), 389-410.

Tsonos, A.G. (2007), "Cyclic load behavior of reinforced concrete beam-column subassemblages of modern structures", *ACI Struct. J.* **104**(4), 468-478.

Uma, S.R. and Prasad, A.M. (2003), "Analytical model for beam column joint in RC frames under seismic conditions", *J. Struct. Eng., SERC, India*, **30**(3), 163-171.

Uma, S.R. and Prasad, A.M. (2006), "Seismic behavior of beam-column joints in RC moment resisting frames: a review", *Indian Conc. J.*, January, 33-42.

Uzumeri, S.M. (1977), "Strength and ductility of cast-in-place beam-column joints", *ACI, SP 53-12(Reinforced Concrete in Seismic Zones)*, Detroit, 293-350.

Wallace, J.W., McConnell, S.W., Gupta, P., and Cote, P.A. (1998), "Use of headed reinforcement in beam-column joints subjected to earthquake loads", *ACI Struct. J.*, **95**(5), 590-606.

Notations

a	: depth from the top fibre up to which the tensile stress in concrete is assumed as uniform.
A^h_{core}	: horizontal cross-sectional area of the joint core resisting the horizontal shear force.
A_g	: gross cross sectional area of column
A_{st}	: steel area
b	: breadth of beam
C	: force in the bottom steel
D_c	: total depth of beam
d_b	: effective depth of beam
f'_c	: cylinder strength of concrete
f_{ck}	: characteristic cube strength of concrete
f_{cr}	: modulus of rupture of concrete
f_t	: maximum tensile stress of concrete
f'_t	: tensile stress at any point in a plane of concrete section
h	: overall depth of beam
k	: stress reduction factor
L	: lever arm for P
L_b	: length of beam
L_c	: length of column

M : bending moment causing failure of concrete
P : Load acting at the free end of the cantilever,
P_u : ultimate load
P_{u1} : ultimate load computed by proposed equation
P_{u2} : ultimate load computed by principal stress theory
P_{ucon} : concrete contribution to the ultimate load.
P_{ue} : ultimate load obtained from experiment
P_{yc} : yield load computed
P_{ye} : yield load obtained from experiment
P_{ys} : yield load of steel
t : effective cover
T : tensile yield force in top steel
T_c : tensile force in concrete
V_s : dowel force in steel plus shear in concrete
Z : modulus of section
σ_1 : principal tensile stress in concrete
σ_y : yield stress of steel
σ_s : stress in bottom steel
τ_{jh} : horizontal shear stress of joint
γ : factor γ depends on the confinement provided by the members framing in to the joint
Φ : diameter of reinforcement bar